Results in Physics 19 (2020) 103581

Contents lists available at ScienceDirect

Results in Physics

journal homepage: www.elsevier.com/locate/rinp

Dynamics of two-mode Sawada-Kotera equation: Mathematical and graphical analysis of its dual-wave solutions

Dipankar Kumar [a], Choonkil Park [b,*], Nishat Tamanna [a], Gour Chandra Paul [c,*], M.S. Osman [d,e,*]

[a] Department of Mathematics, Bangabandhu Sheikh Mujibur Rahman Science and Technology University, Gopalganj 8100, Bangladesh
[b] Research Institute for Natural Sciences, Hanyang University Seoul 04763, South Korea
[c] Department of Mathematics, University of Rajshahi, Rajshahi 6205, Bangladesh
[d] Department of Mathematics, Faculty of Science, Cairo University, Giza, Egypt
[e] Department of Mathematics, Faculty of Applied Science, Umm Alqura University, Makkah 21955, Saudi Arabia

ARTICLE INFO

Keywords:
Two-mode Sawada-Kotera equation
The modified Kudryashov method
The new auxiliary equation method
Dual-wave solitons

ABSTRACT

New dual-wave soliton solutions are addressed for the two-mode Sawada-Kotera (TmSK) equation arising in fluids by the modified Kudryashov and new auxiliary equation methods. As outcomes, bright, dark, periodic, and singular-periodic dual-wave solutions are obtained. The graphs of the solutions are provided to show the impact of the parameters. A comparison between our solutions and the existing ones is carried out.

Introduction

It is well recognized that two-mode nonlinear partial differential equations (PDEs) are the extended form of standard mode PDEs. Both types of PDEs play the considerable role to explain the pragmatic phenomena in various fields [1] by investigating their analytic and numerical solutions. Before the invention of symbolic computation software such as Maple, Mathematica, MATLAB, etc., it was challenging to determine analytic and numerical solutions of nonlinear PDEs. Nowadays, it is comfortable, but important to solve such types of nonlinear PDEs via analytic, semi-analytic, and numerical methods due to the advancement of symbolic computation software. Mostly, during the nineteenth centuries, the diverse standard mode nonlinear PDEs have been introduced by several researchers and various types of wave solutions have been constructed via several analytic, semi-analytic, and numerical methods efficiently viz. the Kudryashov method [2], the modified Kudryashov method [3–5], the generalized Kudryashov method [6,7], the extended Kudryashov method [8], the trial equation method [9], the extended trial equation method [10], the nth Bäcklund transformation (BT) [11–13], the modified simple equation method [14], the sine-Gordon equation expansion method [15,16], the extended sinh-Gordon equation expansion method [16–18], the extended simplest equation method [19], the new extended direct algebraic method [20], the unified method and its extended form [21–24], the generalized unified method [25], the new auxiliary equation expansion method [26], the successive differentiation method [27], the Adomian decomposition method [28], the Hirota bilinear method [29–35], the wavelet method [36], the finite difference method [37], the finite element method [38], and other techniques [39–43].

Recently, a new family of nonlinear PDEs under the name "two-mode" or "dual-mode" have been established regarding temporal and spatial derivatives. Regarding this interest, researchers have been recognized some two-mode nonlinear PDEs viz. two-mode KdV (TmKdV) [44,45], two-mode mKdV (TmmKdV) [46,47], two-mode fifth-order KdV (TmfKdV) [48,49], two-mode Sharma-Tasso-Olver (TmSTO) [50], two-mode Burgers' (TmB) [51], two-mode KdV-Burgers' (TmKdV-B) [52], two-mode perturbed Burgers' (TmPB) [53], two-mode Ostrovsky (TmO) [53], two-mode Kadomtsev-Petviashvili (TmKP) [54,55], two-mode Kuramoto-Sivashinsky (TmKS) [56], two-mode dispersive Fisher (TmF) [57], two-mode Boussinesq-Burgers (TmBB) [58], two-mode nonlinear Schrödinger (TmNLS) [59], two-mode coupled KdV (TmCKdV) [60], two-mode coupled mKdV (TmCmKdV) [61], and two-mode Hirota-Satsuma coupled KdV (TmHSC-KdV) [62] equations and the concerning dual-wave solutions are constructed by different analytical approaches. Among these methods the (G'/G)-expansion method, the tanh expansion method, the Kudryshov method, the rational sine-cosine method, the simplified Hirota's method, the sech-csch method, the tanh-coth method, the sinh-cosh method, the

* Corresponding authors at: Department of Mathematics, Faculty of Science, Cairo University, Giza, Egypt (M.S. Osman); Research Institute for Natural Sciences, Hanyang University Seoul 04763, South Korea (C. Park); Department of Mathematics, University of Rajshahi, Rajshahi 6205, Bangladesh (G.C. Paul).

E-mail addresses: baak@hanyang.ac.kr (C. Park), pcgour2001@yahoo.com (G.C. Paul), mofatzi@sci.cu.edu.eg (M.S. Osman).

https://doi.org/10.1016/j.rinp.2020.103581
Received 5 October 2020; Received in revised form 23 October 2020; Accepted 31 October 2020
Available online 6 November 2020

trigonometric function method, the Fourier spectral method, the Bäcklund transformation, and different other methods [39–65]. As outcomes, some soliton-kink, multiple solitons-kink, bright, dark, and singular-periodic wave solutions have been carried out to the aforesaid equations.

In 2019, Wazwaz [48] developed two-mode Sawada-Kotera (TmSK) equation from the two-mode fifth-order KdV (TmfKdV) equation and determined some multiple soliton solutions via the simplified Hirota method. Later, Akbar et al. [49] studied the TmfKdV equation and constructed some bright, kink, and singular periodic solutions through the Kudryashov and sine-cosine function methods. It is to be noted that the TmSK equation is a particular case of the TmfKdV equation. To the best of authors' knowledge, despite extensive studies on some dual mode PDEs, the contributions to the aforesaid TmSK equation are limited. It is manifested from the literature point of view that there are some scopes for further investigations on the TmSK equation to construct new dual-wave solutions via the modified Kudryashov method (mKM) and the new auxiliary equation method (NAEM) as well as to draw their physical clarifications. It is of interest to note here that the Kudryashov method is a special case of the mKM, and the mKM is also a particular case of NAEM. Thus, motivated by the existing literature, a modest effort has been made in this study to construct some new dual-wave solutions to the TmSK equation via the mKM and NAEM. The solutions attained by the mKM and NAEM are to be new in the sense of methods application.

The rest of the paper is organized as follows. In Section "Formulation of dual/two-mode equations", an overview of the general form of two-mode standard equation and TmSK equation are provided. In Section "Reviews of the methods", the reviews of the mKM and NAEM are described. The outcomes from the investigation are presented in Section "Construction of dual-wave solutions: mathematical analysis". In Section "Discussion and the graphical analysis of the dual-wave solutions", a general discussion and some of the graphical illustrations of the acquired solutions are presented. At the end, conclusions and future recommendations of the paper are exposed in Section "Conclusions and future recommendations".

Formulation of dual/two-mode equations

General form of two-mode standard equation

The general form of two-mode equation proposed by Korsunsky [44], is given as

$$u_{tt} - s^2 u_{xx} + \left(\frac{\partial}{\partial t} - \alpha s \frac{\partial}{\partial x}\right) N(u, uu_x, \cdots) + \left(\frac{\partial}{\partial t} - \beta s \frac{\partial}{\partial x}\right) L(u_{rx}, r \geq 2) = 0, \tag{1}$$

Eq. (1) is established from the standard mode equation: $u_t + N(u, uu_x, \cdots) + L(u_{rx}, r \geq 2) = 0$. In Eq. (1), $u(x,t)$ is an unknown function, where $(x,t) \in (-\infty, \infty)$, $s > 0$is the phase velocity, $|\beta| \leq 1$, $|\alpha| \leq 1$, α, β represent the nonlinearity parameter and dispersion parameter, respectively, and $N(u, uu_x, \cdots)$ and $L(u_{rx}, r \geq 2)$ indicate the nonlinear and linear terms, respectively.

Two-mode Sawada-Kotera (SK) equation

The standard SK equation reads [48]

$$u_t + \left(\frac{5}{3}u^3 + 5uu_{xx}\right)_x + u_{xxxxx} = 0 \tag{2}$$

with linear term u_{xxxxx} and nonlinear term $\left(\frac{5}{3}u^3 + 5uu_{xx}\right)_x$.

Combining the sense of Korsunsky [44], following Wazwaz [48], the two-mode SK(TmSK) equation of the standard SK equation specified by Eq. (2) is given by

$$u_{tt} - s^2 u_{xx} + \left(\frac{\partial}{\partial t} - \alpha s \frac{\partial}{\partial x}\right)\left(\frac{5}{3}u^3 + 5uu_{xx}\right)_x + \left(\frac{\partial}{\partial t} - \beta s \frac{\partial}{\partial x}\right) u_{xxxxx} = 0 \tag{3}$$

It is obvious that for $s = 0$, the TmSK equation specified by Eq. (3) after integrating regarding time t is reduced to the standard mode SK equation given by Eq. (2). Eq. (3) describes the propagation of moving two-waves under the influence of phase velocity (s), dispersion (β), and nonlinearity (α) factors.

Reviews of the methods

The general form of nonlinear PDEs can be written as

$$F(u, u_x, uu_x, u_t, u_{xx}, uu_{xx}, u_{tt}, \cdots\cdots) = 0, \tag{4}$$

where F is a polynomial function with respect to some specified independent variables x, t, and $u = u(x,t)$ is an unknown function.

By introducing the transformation $u(x,t) = u(\xi)$, where $\xi = x - vt$, Eq. (4) can be converted into the following ordinary differential equation (ODE):

$$P(u, u^{'}, u^{''}, uu^{''}, \cdots\cdots\cdots) = 0, \tag{5}$$

where P is a polynomial of u and its derivatives, and the superscripts stand for ordinary derivatives with respect to ξ.

The modified Kudryashov method

In this section a brief overview of the mKM [3] is presented.

Let us assume that the solution $u(\xi)$ of Eq. (5) can be set as

$$u(\xi) = a_0 + \sum_{i=1}^{N} a_i Q^i(\xi), \tag{6}$$

where the arbitrary constants $a_i (i = 1, 2, \cdots\cdots, N)$ are determined later, but $a_N \neq 0$ and N is a positive integer that can be determined via the homogeneous balance principle by balancing between the nonlinear terms and highest derivatives of Eq. (5). The function $Q(\xi)$ of Eq. (6) satisfies the following ODE:

$$Q^{'}(\xi) = \left(Q^2(\xi) - Q(\xi)\right) ln(a), \tag{7}$$

where $a > 1$ and the general solution of Eq. (7) is $Q(\xi) = \frac{1}{1+da^{\xi}}$, $d \neq 0$.

By inserting Eq. (6) along with Eq. (7) into Eq. (5) and equating the coefficients of the powers of $Q^i(\xi)$ to zero, we get a system of algebraic equations in parameters a_0, a_1 and v. Setting the obtained value in Eq. (6), one can finally generate new exact solutions for Eq. (4).

The new auxiliary equation method (NAEM)

In this section a brief overview of the NAEM [26] is presented.

As per the NAEM, the exact solution of Eq. (5) is supposed to have the following form:

$$u(\xi) = \sum_{i=0}^{N} c_i a^{\{if(\xi)\}}, \tag{8}$$

where $c_0, c_1, \cdots, c_N$ are constants to be calculated such that $c_N \neq 0$ and the positive integer N can be determined by balancing the nonlinear terms and highest derivatives in Eq. (8). The function $f(\xi)$ of Eq. (8) satisfies the following ODE [26]:

$$f^{'}(\xi) = \frac{1}{\ln(a)}\left\{pa^{-f(\xi)} + q + ra^{f(\xi)}\right\} \tag{9}$$

By inserting Eq. (8) with the value of N along with Eq. (9) into Eq. (5) and collecting all terms having powers of $a^{if(\xi)}, (i = 0, 1, 2, \cdots)$ to zero, a system of algebraic equation is attained, which on solving gives the values of c_i's, v, and etc. Finally, plugging the values of c_i's, v and the solutions of Eq. (9) into Eq. (8), one can generate the abundant dual-wave solutions of Eq. (4).

The solutions of Eq. (9) are obtained as follows [26]:

Family 1: When $q^2 - 4pr < 0$ and $r \neq 0$,

$$a^{f(\xi)} = \frac{-q}{2r} + \frac{\sqrt{4pr - q^2}}{2r} tan\left(\frac{\sqrt{4pr - q^2}}{2}\xi\right), \tag{10}$$

$$a^{f(\xi)} = \frac{-q}{2r} - \frac{\sqrt{4pr - q^2}}{2r} cot\left(\frac{\sqrt{4pr - q^2}}{2}\xi\right) \tag{11}$$

Family 2: When $q^2 - 4pr > 0$ and $r \neq 0$,

$$a^{f(\xi)} = \frac{-q}{2r} - \frac{\sqrt{q^2 - 4pr}}{2r} tanh\left(\frac{\sqrt{q^2 - 4pr}}{2}\xi\right), \tag{12}$$

$$a^{f(\xi)} = \frac{-q}{2r} - \frac{\sqrt{q^2 - 4pr}}{2r} coth\left(\frac{\sqrt{q^2 - 4pr}}{2}\xi\right) \tag{13}$$

Family 3: When $q^2 + 4p^2 < 0$, $r \neq 0$ and $r = -p$,

$$a^{f(\xi)} = \frac{q}{2p} - \frac{\sqrt{-4p^2 - q^2}}{2p} tan\left(\frac{\sqrt{-4p^2 - q^2}}{2}\xi\right), \tag{14}$$

$$a^{f(\xi)} = \frac{q}{2p} + \frac{\sqrt{-4p^2 - q^2}}{2p} cot\left(\frac{\sqrt{-4p^2 - q^2}}{2}\xi\right) \tag{15}$$

Family 4: When $q^2 + 4p^2 > 0$, $r \neq 0$ and $r = -p$,

$$a^{f(\xi)} = \frac{q}{2p} + \frac{\sqrt{4p^2 + q^2}}{2p} tanh\left(\frac{\sqrt{4p^2 + q^2}}{2}\xi\right), \tag{16}$$

$$a^{f(\xi)} = \frac{q}{2p} + \frac{\sqrt{4p^2 + q^2}}{2p} coth\left(\frac{\sqrt{4p^2 + q^2}}{2}\xi\right) \tag{17}$$

Family 5: When $q^2 - 4p^2 < 0$ and $r = p$,

$$a^{f(\xi)} = \frac{-q}{2p} + \frac{\sqrt{4p^2 - q^2}}{2p} tan\left(\frac{\sqrt{4p^2 - q^2}}{2}\xi\right), \tag{18}$$

$$a^{f(\xi)} = \frac{-q}{2p} - \frac{\sqrt{4p^2 - q^2}}{2p} cot\left(\frac{\sqrt{4p^2 - q^2}}{2}\xi\right) \tag{19}$$

Family 6: When $q^2 - 4p^2 > 0$ and $r = p$,

$$a^{f(\xi)} = \frac{-q}{2p} - \frac{\sqrt{-4p^2 + q^2}}{2p} tanh\left(\frac{\sqrt{-4p^2 + q^2}}{2}\xi\right) \tag{20}$$

$$a^{f(\xi)} = \frac{-q}{2p} - \frac{\sqrt{-4p^2 + q^2}}{2p} coth\left(\frac{\sqrt{-4p^2 + q^2}}{2}\xi\right) \tag{21}$$

Family 7: When $q^2 = 4pr$,

$$a^{f(\xi)} = -\frac{2 + q\xi}{2r\xi} \tag{22}$$

Family 8: When $rp < 0, q = 0$ and $r \neq 0$,

$$a^{f(\xi)} = -\sqrt{\frac{-p}{r}} tanh\left(\sqrt{-rp}\,\xi\right) \tag{23}$$

$$a^{f(\xi)} = -\sqrt{\frac{-p}{r}} coth\left(\sqrt{-rp}\,\xi\right) \tag{24}$$

Family 9: When $q = 0$ and $p = -r$,

$$a^{f(\xi)} = \frac{1 + e^{-2r\xi}}{-1 + e^{-2r\xi}} \tag{25}$$

Family 10: When $p = r = 0$,

$$a^{f(\xi)} = \cosh(q\xi) + \sinh(q\xi) \tag{26}$$

Family 11: When $p = q = K$ and $r = 0$,

$$a^{f(\xi)} = e^{K\xi} - 1 \tag{27}$$

Family 12: When $r = q = K$ and $p = 0$,

$$a^{f(\xi)} = \frac{e^{K\xi}}{1 - e^{K\xi}} \tag{28}$$

Family 13: When $q = p + r$,

$$a^{f(\xi)} = -\frac{1 - pe^{(p-r)\xi}}{1 - re^{(p-r)\xi}} \tag{29}$$

Family 14: When $q = -(p + r)$,

$$a^{f(\xi)} = \frac{p - e^{(p-r)\xi}}{r - e^{(p-r)\xi}} \tag{30}$$

Family 15: When $p = 0$,

$$a^{f(\xi)} = \frac{qe^{q\xi}}{1 - re^{q\xi}} \tag{31}$$

Family 16: When $q = p = r \neq 0$,

$$a^{f(\xi)} = \frac{1}{2}\left\{\sqrt{3}\tan\left(\frac{\sqrt{3}}{2}p\xi\right) - 1\right\} \tag{32}$$

Family 17: When $q = r = 0$,

$$a^{f(\xi)} = p\xi \tag{33}$$

Family 18: When $q = p = 0$,

$$a^{f(\xi)} = -\frac{1}{r\xi} \tag{34}$$

Family 19: When $p = r$ and $q = 0$,

$$a^{f(\xi)} = \tan(p\xi) \tag{35}$$

Family 20: When $r = 0$,

$$a^{f(\xi)} = e^{q\xi} - \frac{m}{n} \tag{36}$$

Construction of dual-wave solutions: mathematical analysis

In this section, we will construct dual-wave solutions to the TmSK equation specified by Eq. (3) via the method described in Section "Reviews of the methods".

In order to covert the PDE specified by Eq. (3) into ODE, we use the following transformation as $\xi = kx - ct$. By using the specified transformation into Eq. (3), we get an ODE as follows.

$$\left(-k^2s^2+c^2\right)u'' - k\alpha s\left(10kuu'^2+5ku^2u''+5k^3\left(u''\right)^2+10k^3u'u'''+5k^3u''''u\right) - 5c\left(2kuu'^2+ku^2u''+k^3u''^2+2k^3u'u'''+k^3u''''u\right) - k^5cu'''''' - \beta sk^6u'''''' = 0. \tag{37}$$

Application of the modified Kudryashov method

The index N is to be determined by applying the homogenous balance procedure with the linear term u'''''' against the nonlinear term u^2u'' in Eq. (37), which gives $N = 2$. Therefore, Eq. (6) takes the following form:

$$u(\xi) = a_0 + a_1 Q(\xi) + a_2 Q^2(\xi) \tag{38}$$

A direct substitution of Eq. (38) along with Eq. (7) and $\alpha = \beta$ into Eq. (37) via the symbolic computation software Maple, and equating the coefficients of $Q^r(\xi), (r = 1, 2, \cdots, 8)$to zero a set of algebraic equations involving a_0, a_1, a_2, c, is attained. Solving the attained system of equations via the mentioned symbolic computation software, the following solution sets are obtained:

Set 1:

$a_0 = -ln(a)^2k^2, a_1 = 12ln(a)^2k^2, a_2 = -12ln(a)^2k^2$, and

$$c = \left(\frac{1}{2}ln(a)^4k^4 \pm \frac{1}{2}\sqrt{ln(a)^8k^8 + 4s\beta ln(a)^4k^4 + 4s^2}\right)k$$

Set-2:

$$a_0 = -\frac{1}{10}\frac{1}{k(ks\beta+c)}\left(5s\beta ln(a)^2k^4 + 5ck^3ln(a)^2 \mp \left(5ln(a)^4k^8s^2\beta^2 + 10ln(a)^4ck^7s\beta + 5ln(a)^4k^6c^2 - 20k^4s^3\beta + 20c^2k^2s\beta - 20ck^3s^2 + 20c^3k\right)^{\frac{1}{2}}\right), a_1 = 6ln(a)^2k^2$$

, and

$a_2 = -6ln(a)^2k^2$

Plugging Set-1 and Set-2 along with the solution of Eq. (7) into Eq. (38), one can produce the following solutions:

$$u_{1,2}(x,t) = -k^2ln(a)^2 + \frac{12k^2ln(a)^2}{1+da^{-\left(\frac{1}{2}ln(a)^4k^4 \pm \frac{1}{2}\sqrt{ln(a)^8k^8+4s\beta ln(a)^4k^4+4s^2}\right)kt+kx}} - \frac{12k^2ln(a)^2}{\left(1+da^{-\left(\frac{1}{2}ln(a)^4k^4 \pm \frac{1}{2}\sqrt{ln(a)^8k^8+4s\beta ln(a)^4k^4+4s^2}\right)kt+kx}\right)^2}, \tag{39}$$

$$u_{3,4}(x,t) = -\frac{1}{10}\frac{1}{k(ks\beta+c)}\left(5s\beta ln(a)^2k^4 + 5ck^3ln(a)^2 \mp \left(5ln(a)^4k^8s^2\beta^2 + 10ln(a)^4ck^7s\beta + 5ln(a)^4k^6c^2 - 20k^4s^3\beta + 20c^2k^2s\beta - 20ck^3s^2 + 20c^3k\right)^{\frac{1}{2}}\right) + \frac{6k^2ln(a)^2}{1+da^{-ct+kx}} - \frac{6k^2ln(a)^2}{\left(1+da^{-ct+kx}\right)^2}. \tag{40}$$

Application of the new auxiliary equation method

In order to determine a series of dual-wave solutions of TmSK equation by the NAEM, the finite expansion of NAEM formal solution can be assumed to Eq. (3) as follows

$$u(\xi) = a_0 + a_1 a^{f(\xi)} + a_2\left(a^{f(\xi)}\right)^2, \tag{41}$$

By plugging Eq. (41) along with Eq. (9) and $\alpha = \beta$ into Eq. (37) via Maple symbolic computation software, and equating the coefficients of $\left(a^{f(\xi)}\right)^r, (r = 1, 2, \cdots, 9)$to zero a set of algebraic equations involving a_0, a_1, a_2, c, is attained. Solving the obtained set of algebraic equations with the aid of Maple yields:

$a_0 = -(8pr+q^2)k^2, a_1 = -12k^2qr, a_2 = -12k^2r^2$, and c

$$= \left(8p^2k^4r^2 - 4q^2k^4pr + \frac{1}{2}q^4k^4 \pm \frac{1}{2}\sqrt{256k^8p^4r^4 - 256p^3k^8q^2r^3 + 96p^2k^8r^2q^4 - 16q^6k^8pr + q^8k^8} \pm \frac{1}{2}\sqrt{64p^2k^4r^2s\beta - 32s\beta k^4prq^2 + 4q^4k^4s\beta + 4s^2}\right)k$$

.

Substituting the values of a_0, a_1, a_2, and c into Eq. (41), the following class of solution is determined:

$$u(\xi) = -\left(8pr+q^2\right)k^2 - 12k^2qr\left(a^{f(\xi)}\right) - 12k^2r^2\left(a^{f(\xi)}\right)^2, \tag{42}$$

By putting the solutions of auxiliary equation specified by Eq. (9) (Family-1 to Family-20) into Eq. (42), the following solutions are retrieved:

For Family 1: When $q^2 - 4pr < 0$ and $r \neq 0$,

$$u_{1,2}(x,t) = -\left(8pr+q^2\right)k^2 - 12k^2qr\left(-\frac{q}{2r} + \frac{1}{2r}\sqrt{4pr-q^2}\tan\left(\frac{\sqrt{4pr-q^2}}{2}\xi\right)\right) - 12k^2r^2\left(-\frac{q}{2r} + \frac{1}{2r}\sqrt{4pr-q^2}\tan\left(\frac{\sqrt{4pr-q^2}}{2}\xi\right)\right)^2, \tag{43}$$

$$u_{3,4}(x,t)=-\left(8pr+q^2\right)k^2-12k^2qr\left(-\frac{q}{2r}-\frac{1}{2r}\sqrt{4pr-q^2}cot\left(\frac{\sqrt{4pr-q^2}}{2}\xi\right)\right)-12k^2r^2\left(-\frac{q}{2r}-\frac{1}{2r}\sqrt{4pr-q^2}cot\left(\frac{\sqrt{4pr-q^2}}{2}\xi\right)\right)^2. \tag{44}$$

For Family 2: When $\mathbf{q}^2-4\mathbf{pr}>0$ and $\mathbf{r}\neq 0$,

$$u_{5,6}(x,t)=-(8pr+q^2)k^2-12k^2qr\left(\frac{-q}{2r}-\frac{\sqrt{q^2-4pr}}{2r}tanh\left(\frac{\sqrt{q^2-4pr}}{2}\xi\right)\right)-12k^2r^2\left(\frac{-q}{2r}-\frac{\sqrt{q^2-4pr}}{2r}tanh\left(\frac{\sqrt{q^2-4pr}}{2}\xi\right)\right)^2 \tag{45}$$

$$u_{7,8}(x,t)=-\left(8pr+q^2\right)k^2-12k^2qr\left(\frac{-q}{2r}-\frac{\sqrt{q^2-4pr}}{2r}coth\left(\frac{\sqrt{q^2-4pr}}{2}\xi\right)\right)-12k^2r^2\left(\frac{-q}{2r}-\frac{\sqrt{q^2-4pr}}{2r}coth\left(\frac{\sqrt{q^2-4pr}}{2}\xi\right)\right)^2 \tag{46}$$

For Family 3: When $\mathbf{q}^2+4\mathbf{p}^2<0$, $\mathbf{r}\neq 0$ and $\mathbf{r}=-\mathbf{p}$,

$$u_{9,10}(x,t)=-\left(8pr+q^2\right)k^2-12k^2qr\left(\frac{q}{2p}-\frac{\sqrt{-4p^2-q^2}}{2p}tan\left(\frac{\sqrt{-4p^2-q^2}}{2}\xi\right)\right)-12k^2r^2\left(\frac{q}{2p}-\frac{\sqrt{-4p^2-q^2}}{2p}tan\left(\frac{\sqrt{-4p^2-q^2}}{2}\xi\right)\right)^2 \tag{47}$$

$$u_{11,12}(x,t)=-\left(8pr+q^2\right)k^2-12k^2qr\left(\frac{q}{2p}+\frac{\sqrt{-4p^2-q^2}}{2p}cot\left(\frac{\sqrt{-4p^2-q^2}}{2}\xi\right)\right)-12k^2r^2\left(\frac{q}{2p}+\frac{\sqrt{-4p^2-q^2}}{2p}cot\left(\frac{\sqrt{-4p^2-q^2}}{2}\xi\right)\right)^2. \tag{48}$$

For Family 4: When $\mathbf{q}^2+4\mathbf{p}^2>0$, $\mathbf{r}\neq 0$ and $\mathbf{r}=-\mathbf{p}$,

$$u_{13,14}(x,t)=-\left(8pr+q^2\right)k^2-12k^2qr\left(\frac{q}{2p}+\frac{\sqrt{4p^2+q^2}}{2p}tanh\left(\frac{\sqrt{4p^2+q^2}}{2}\xi\right)\right)-12k^2r^2\left(\frac{q}{2p}+\frac{\sqrt{4p^2+q^2}}{2p}tanh\left(\frac{\sqrt{4p^2+q^2}}{2}\xi\right)\right)^2 \tag{49}$$

$$u_{15,16}(x,t)=-\left(8pr+q^2\right)k^2-12k^2qr\left(\frac{q}{2p}+\frac{\sqrt{4p^2+q^2}}{2p}coth\left(\frac{\sqrt{4p^2+q^2}}{2}\xi\right)\right)-12k^2r^2\left(\frac{q}{2p}+\frac{\sqrt{4p^2+q^2}}{2p}coth\left(\frac{\sqrt{4p^2+q^2}}{2}\xi\right)\right)^2 \tag{50}$$

For Family 5: When $q^2-4p^2<0$ and $r=p$,

$$u_{17,18}(x,t)=-\left(8pr+q^2\right)k^2-12k^2qr\left(\frac{-q}{2p}+\frac{\sqrt{4p^2-q^2}}{2p}tan\left(\frac{\sqrt{4p^2-q^2}}{2}\xi\right)\right)-12k^2r^2\left(\frac{-q}{2p}+\frac{\sqrt{4p^2-q^2}}{2p}tan\left(\frac{\sqrt{4p^2-q^2}}{2}\xi\right)\right)^2, \tag{51}$$

$$u_{19,20}(x,t)=-\left(8pr+q^2\right)k^2-12k^2qr\left(\frac{-q}{2p}-\frac{\sqrt{4p^2-q^2}}{2p}cot\left(\frac{\sqrt{4p^2-q^2}}{2}\xi\right)\right)-12k^2r^2\left(\frac{-q}{2p}-\frac{\sqrt{4p^2-q^2}}{2p}cot\left(\frac{\sqrt{4p^2-q^2}}{2}\xi\right)\right)^2 \tag{52}$$

For Family 6: When $q^2-4p^2>0$ and $r=p$,

$$u_{21,22}(x,t)=-\left(8pr+q^2\right)k^2-12k^2qr\left(\frac{-q}{2p}-\frac{\sqrt{-4p^2+q^2}}{2p}tanh\left(\frac{\sqrt{-4p^2+q^2}}{2}\xi\right)\right)-12k^2r^2\left(\frac{-q}{2p}-\frac{\sqrt{-4p^2+q^2}}{2p}tanh\left(\frac{\sqrt{-4p^2+q^2}}{2}\xi\right)\right)^2, \tag{53}$$

$$u_{23,24}(x,t)=-\left(8pr+q^2\right)k^2-12k^2qr\left(\frac{-q}{2p}-\frac{\sqrt{-4p^2+q^2}}{2p}coth\left(\frac{\sqrt{-4p^2+q^2}}{2}\xi\right)\right)-12k^2r^2\left(\frac{-q}{2p}-\frac{\sqrt{-4p^2+q^2}}{2p}coth\left(\frac{\sqrt{-4p^2+q^2}}{2}\xi\right)\right)^2. \tag{54}$$

For Family 7: When $q^2=4pr$,

$$u_{25,26}(x,t)=-\left(8pr+q^2\right)k^2-12k^2qr\left(-\frac{2+q\xi}{2r\xi}\right)-12k^2r^2\left(-\frac{2+q\xi}{2r\xi}\right)^2 \tag{55}$$

For Family 8: When $rp<0$,$q=0$and $r\neq 0$,

$$u_{27,28}(x,t)=-\left(8pr+q^2\right)k^2-12k^2qr\left(-\sqrt{\frac{-p}{r}}tanh\left(\sqrt{-rp}\xi\right)\right)-12k^2r^2\left(-\sqrt{\frac{-p}{r}}tanh\left(\sqrt{-rp}\xi\right)\right)^2, \tag{56}$$

$$u_{29,30}(x,t)=-\left(8pr+q^2\right)k^2-12k^2qr\left(-\sqrt{\frac{-p}{r}}coth\left(\sqrt{-rp}\,\xi\right)\right)-12k^2r^2\left(-\sqrt{\frac{-p}{r}}coth\left(\sqrt{-rp}\,\xi\right)\right)^2. \tag{57}$$

For Family 9: When $q=0$ and $p=-r$,

$$u_{31,32}(x,t)=-\left(8pr+q^2\right)k^2-12k^2qr\left(\frac{1+e^{-2r\xi}}{-1+e^{-2r\xi}}\right)-12k^2r^2\left(\frac{1+e^{-2r\xi}}{-1+e^{-2r\xi}}\right)^2. \tag{58}$$

For Family 12: When $r = q = K$ and $p = 0$,

$$u_{33,34}(x,t) = -\left(8pr + q^2\right)k^2 - 12k^2qr\left(\frac{e^{K\xi}}{1-e^{K\xi}}\right) - 12k^2r^2\left(\frac{e^{K\xi}}{1-e^{K\xi}}\right)^2. \quad (59)$$

For Family 13: When $q = p + r$,

$$u_{35,36}(x,t) = -\left(8pr + q^2\right)k^2 - 12k^2qr\left(-\frac{1-pe^{(p-r)\xi}}{1-re^{(p-r)\xi}}\right) - 12k^2r^2\left(-\frac{1-pe^{(p-r)\xi}}{1-re^{(p-r)\xi}}\right)^2. \quad (60)$$

For Family 14: When $q = -(p + r)$,

$$u_{37,38}(x,t) = -\left(8pr + q^2\right)k^2 - 12k^2qr\left(\frac{p-e^{(p-r)\xi}}{r-e^{(p-r)\xi}}\right) - 12k^2r^2\left(\frac{p-e^{(p-r)\xi}}{r-e^{(p-r)\xi}}\right)^2 \quad (61)$$

For Family 15: When $p = 0$,

$$u_{39,40}(x,t) = -\left(8pr + q^2\right)k^2 - 12k^2qr\left(\frac{qe^{q\xi}}{1-re^{q\xi}}\right) - 12k^2r^2\left(\frac{qe^{q\xi}}{1-re^{q\xi}}\right)^2. \quad (62)$$

For Family 18: When $q = p = 0$,

$$u_{41,42}(x,t) = -\left(8pr + q^2\right)k^2 - 12k^2qr\left(\frac{-1}{r\xi}\right) - 12k^2r^2\left(\frac{-1}{r\xi}\right)^2. \quad (63)$$

For Family 19: When $p = r$ and $q = 0$,

$$u_{43,44}(x,t) = -\left(8pr + q^2\right)k^2 - 12k^2qr(\tan(p\xi)) - 12k^2r^2(\tan(p\xi))^2. \quad (64)$$

where $\xi = \left(kx - \left(8p^2k^4r^2 - 4q^2k^4pr + \frac{1}{2}q^4k^4 \pm \frac{1}{2}\sqrt{S} \pm \frac{1}{2}\sqrt{T}\right)kt\right)$ for solutions specified by Eqs. (43)–(64), $S = 256k^8p^4r^4 - 256p^3k^8q^2r^3 + 96p^2k^8r^2q^4 - 16q^6k^8pr + q^8k^8$ and $T = 64p^2k^4r^2s\beta - 32s\beta k^4prq^2 + 4q^4k^4s\beta + 4s^2$

Discussion and the graphical analysis of the dual-wave solutions

This section discusses the produced dual-wave solutions and its graphical illustrations for demonstrating the proper physical significance of the TmSK equation arising in fluid dynamics. Regarding this interest, the mKM and NAEM are fruitfully executed to construct numerous types of dual-wave soliton solutions to the aforesaid equation. It is declared earlier that the TmSK equation has been studied via the simplified Hirota method [48], the Kudryashov method [49], and the sine-cosine method [49]. Based on the application of the methods, the authors reported a few numbers of multiple-soliton, bright, kink, and singular-periodic shaped solutions with the restricted conditions $\alpha = \beta = \pm 1$. But in this article, four wave solutions are generated by the mKM and forty-four wave solutions are generated by the NAEM. The explored solutions demonstrate the dual-mode bright, dark, periodic, and singular wave behaviors that are being classified as right/left mode waves. Compared with published results [48,49], it is worth mentioning that the attained dual-wave solutions are new for the applied methods of interest.

In order to understand the proper implication of dual-wave behaviors of the TmSK equation, a few numbers of representative solutions are explained graphically for both the methods. Soliton propagation and collisions of dual-mode waves are discussed analyzing their graphs. To visualize the dual-mode solution's behavior of the attained solutions via mKM given by Eq. (39), the 3D and 2D graphics are presented in Fig. 1

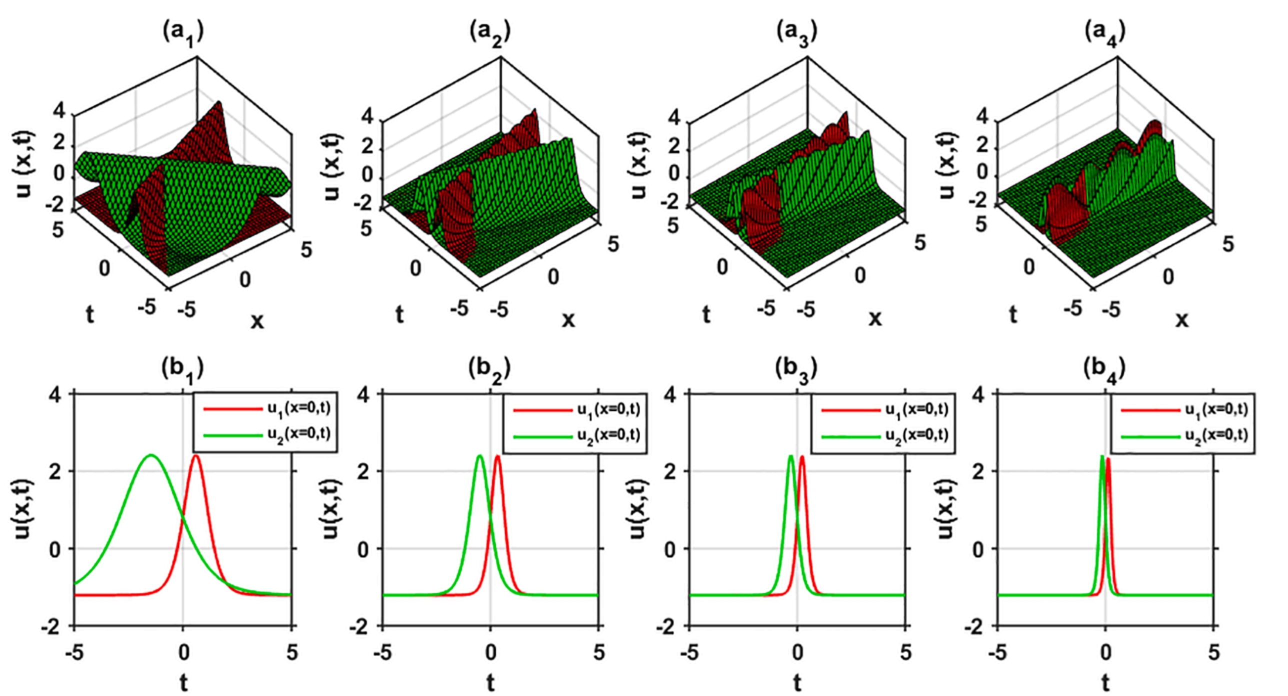

Fig. 1. Three dimensional (3D) plots of the dual wave solutions of u_1 (red color) and u_2 (green color) given by Eq. (39) by taking phase velocities at (a1) $s = 1$, (a2) $s = 3$, (a3) $s = 5$, and (a4) $s = 10$ with upon choice of other free parameter values of $a = 3$, $d = 1$, $k = 1$, and $\beta = 1$. (b1)–(b4): the cross-sectional two-dimensional (2D) plots of (a1–a4) at $x = 0$, respectively. (For interpretation of the references to color in this figure legend, the reader is referred to the web version of this article.)

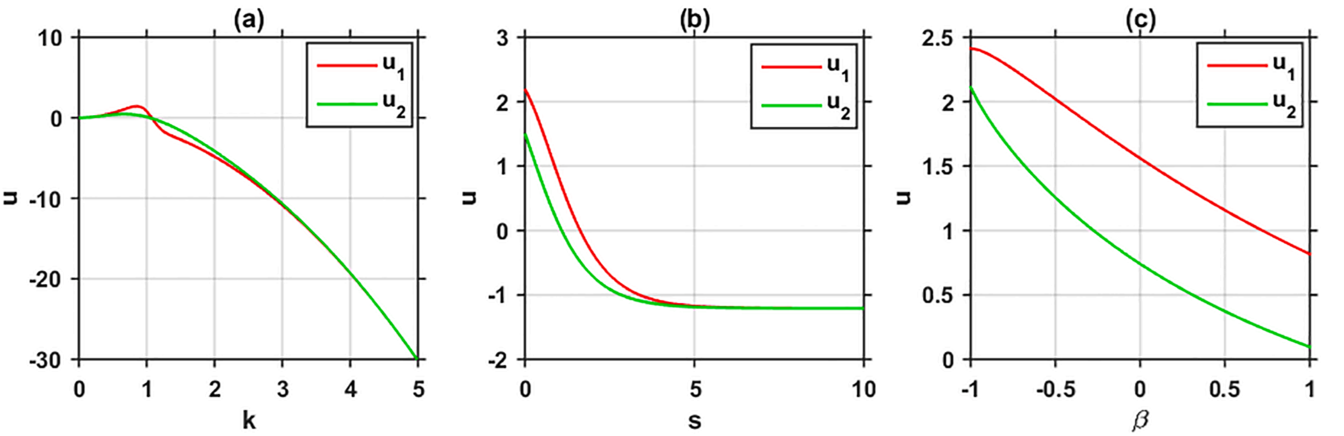

Fig. 2. (a) The effect of wave number (k) when $s = 1$, $\beta = 1$, (b) the effect of phase velocity parameter (s) when $k = 1$, $\beta = 1$, and (c) the effect of dispersion parameter (β) when $k = 1$, $s = 1$ on two-mode waves of u_1 (red color) and u_2 (green color) given by Eq. (39) for $x = 1$, $t = 1$, $a = 3$ and $d = 1$. (For interpretation of the references to color in this figure legend, the reader is referred to the web version of this article.)

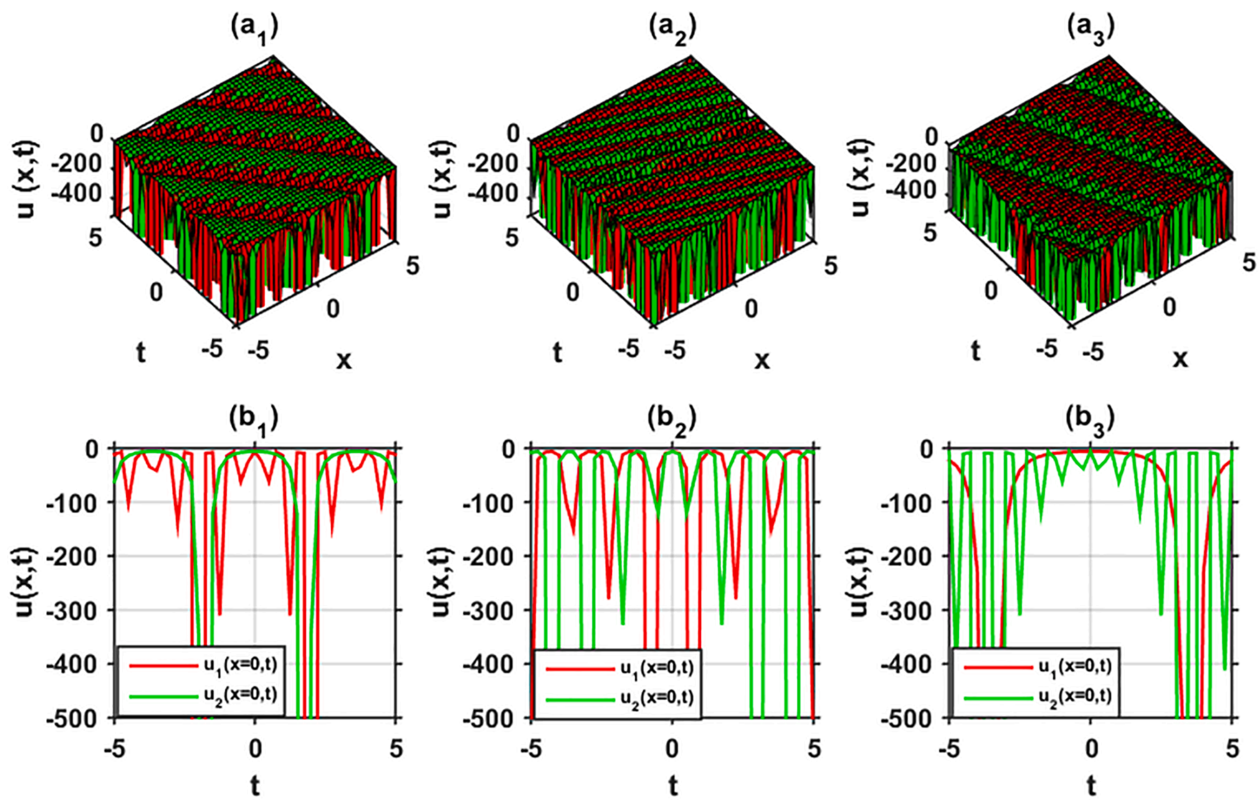

Fig. 3. 3D plots of the dual wave solutions of u_1 (red color) and u_2 (green color) given by Eq. (43) for considering phase velocities at (a1) $s = 1$, (a2) $s = 3$, and (a3) $s = 5$ with upon choice of other free parameter values of $p = 1$, $q = 1$,$r = 1$, $k = 1$, and $\beta = 1$. (b1)–(b3): the cross-sectional 2D plots of (a1)–(a3) at $x = 0$, respectively. (For interpretation of the references to color in this figure legend, the reader is referred to the web version of this article.)

by considering particular values of the free parameters as $a = 3$, $d = 1$, $k = 1$, and $\beta = 1$ for different values of s. Fig. 1(a1)–(a4) present the spatiotemporal variation of the attained solutions of $u_1(x,t)$ and $u_2(x,t)$ for $s = 1,3,5,10$, respectively, that illustrate the bright shaped solitons, whereas Fig. 1(b1)–(b4) show the cross-sectional 2D plots of Fig. 1(a1)–(a4) when $x = 0$. At $s = 1$, it is seen from Fig. 1(a1) that two waves of $u_1(x,t)$ and $u_2(x,t)$ interact with each other. Upon increasing the phase velocity s ($s = 3,5,10$), it is also perceived from Fig. 1(a2)–(a4) that the solitons are colliding with each other and two waves are going to coincide, as well as, the width of each of the two waves is decreasing, but the amplitudes remain unchanged. The above behaviors are clearly justified with the 2D plots given by Fig. 1(b1)–(b4). The impact of k, s and β on the motion of two waves of u_1 and u_2 are displayed in Fig. 2(a)–(c), respectively. It can be seen that from Fig. 2(a) that the profile of u_1 is slightly higher than that of u_2 when k increases from 0 to 1 and then it gradually decreases from 1 to 3, and become stable for remaining k when $x = 1$, $t = 1$, $s = 1$, and $\beta = 1$ are considered. That means, the solutions seem to be dual-wave behavior when $k \in (0,3)$. On the other hand, the profile u_1 is higher than that of u_2 when the phase velocity (s) increases from 0 to 5, and then become stable for other s when $x = 1$, $t = 1$, $k = 1$, and $\beta = 1$ are considered (see Fig. 2(b)). As seen in Fig. 2(c), the profile of u_1 is significantly higher over u_2 for β when $x = 1$, $t = 1$,

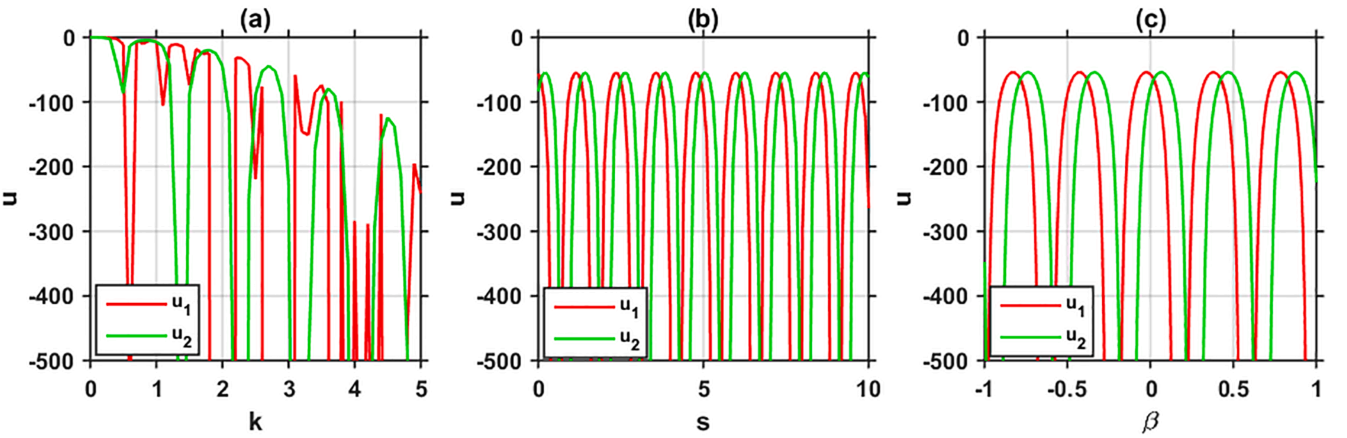

Fig. 4. (a) The effect of wave number (k) when $s = 3$, $\beta = 1$, (b) the effect of phase velocity parameter (s) when $k = 3$, $\beta = 1$, and (c) the effect of dispersion parameter (β) when $k = 3$, $s = 3$ on two-mode waves of u_1 (red color) and u_2 (green color) given by Eq. (43) for $x = 1$, $t = 1$, $p = 1$, $q = 1$,$r = 1$. (For interpretation of the references to color in this figure legend, the reader is referred to the web version of this article.)

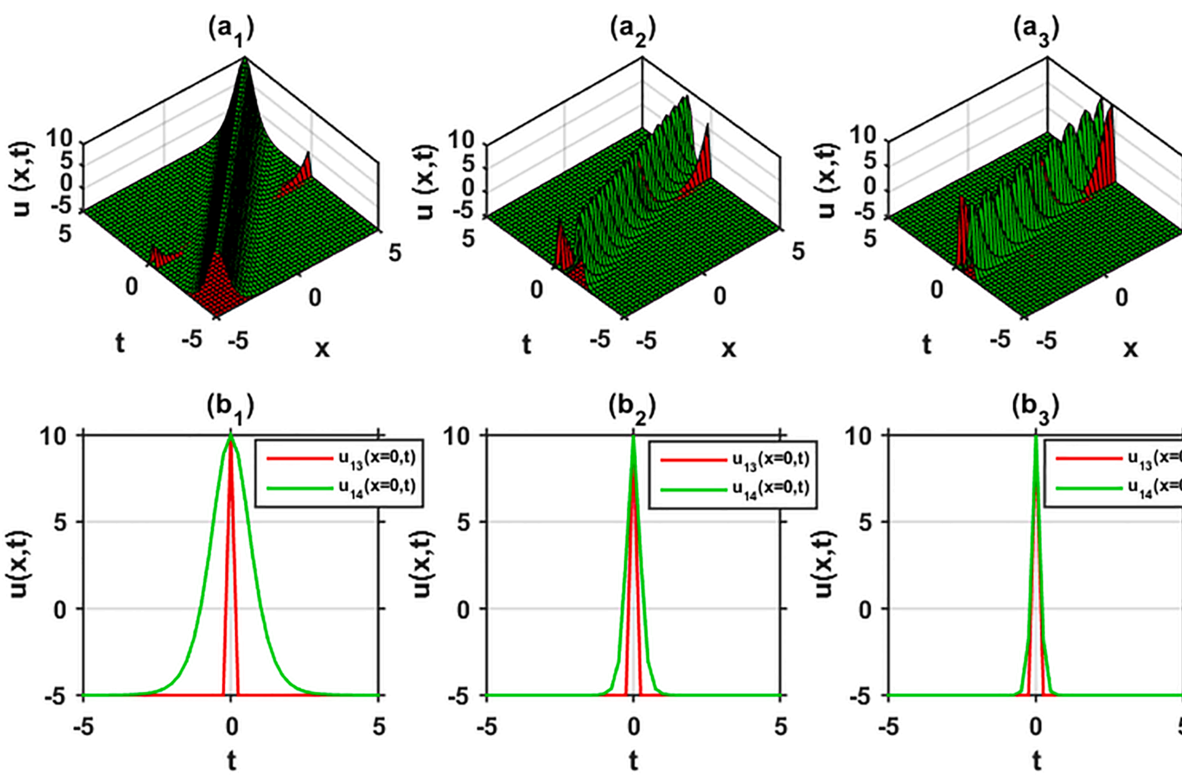

Fig. 5. 3D plots of the dual wave solutions of u_{13} (red color) and u_{14} (green color) given by Eq. (49) for considering phase velocities at (a1) $s = 1$, (a2) $s = 3$, and (a3) $s = 5$ with upon choice of other free parameter values of $p = 1$, $q = -1$,$r = 1$, $k = 1$, and $\beta = -1$. (b1)–(b3): the cross-sectional 2D plots of (a1)–(a3) at $x = 0$, respectively. (For interpretation of the references to color in this figure legend, the reader is referred to the web version of this article.)

$k = 1$, and $s = 1$ are particularly selected. The remaining solutions $u_{3,4}(x,t)$ obtained via the mKM indicate the bright shaped solitons, which are not displayed for the sake of simplicity.

Furthermore, in order to display the dual-mode solutions' behaviors of the attained solutions via the NAEM given by Eq. (43), the 3D and 2D graphics are presented in Fig. 3 by considering particular values of the free parameters as $p = 1$, $q = 1$,$r = 1$, $k = 1$, and $\beta = 1$ for various values of s. Fig. 3(a1)–(a3) present the dynamics of the wave propagation of the two waves of $u_1(x,t)$ and $u_2(x,t)$ upon increasing its phase velocity s, whereas Fig. 3(b1)–(b3) show the cross-sectional 2D plots of Fig. 3(a1)–(a3) when $x = 0$. In such case, it is clear from the Fig. 3 that both solutions demonstrate the periodic shaped solitons colliding with each other. At $s = 1$, it is seen from Fig. 3(a1) that the soliton corresponding to $u_1(x,t)$ shows the smaller period than that of $u_2(x,t)$. As s increases ($s = 3, 5$), one can observe from Fig. 3(a2)–(a3) that the periodicity of $u_1(x,t)$ sequentially decreases, but the periodicity increases for $u_2(x,t)$. The directional changes have been observed for each of the solitons. Such types of behaviors are clearly justified by the 2D plots, which are shown in Fig. 3(b1)–(b3). The role of k, s, and β on the motion of moving two waves of u_1 and u_2 are displayed in Fig. 4(a)–(c), respectively. It is clearly seen from Fig. 4(a)–(c) that the parameters k, s, and β accelerate the direction of motion of the waves and increase or decrease the number of periods.

Fig. 5(a1)–(a3) present the 3D plots of the dual-wave solutions of u_{13}

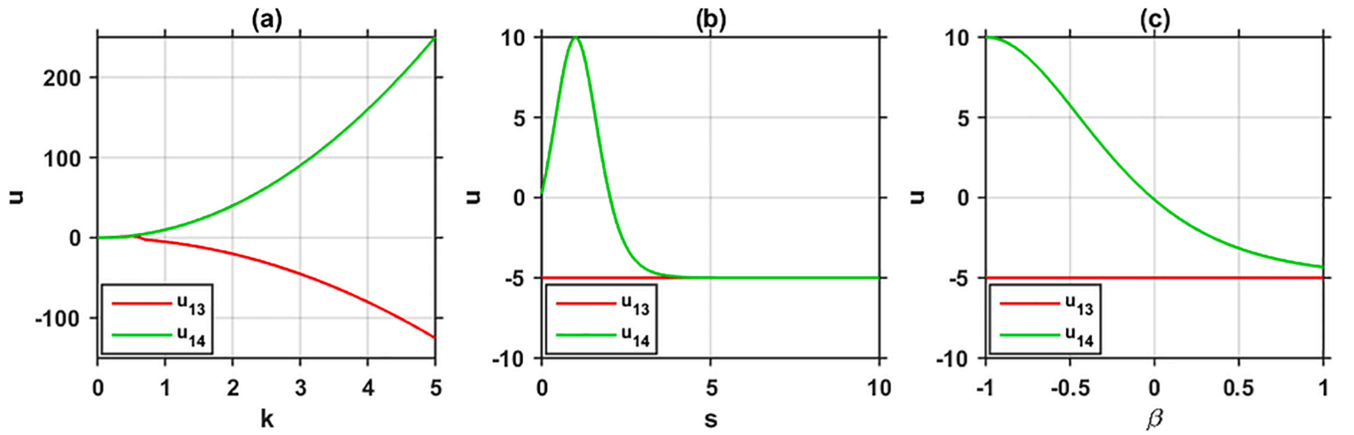

Fig. 6. (a) The effect of wave number (k) when $s = 1$, $\beta = -1$, (b) the effect of phase velocity parameter (s) when $k = 1$, $\beta = -1$, and (c) the effect of dispersion parameter (β) when $k = 1$, $s = 1$ on two-mode waves of u_{13} (red color) and u_{14} (green color) given by Eq. (49) for $x = 1$, $t = 1$, $p = 1$, $q = 1$,$r = -1$. (For interpretation of the references to color in this figure legend, the reader is referred to the web version of this article.)

and u_{14} given by Eq. (49) with phase velocity of $s = 1,3,5$, respectively, along with the consideration of the other parameters, viz. $p = 1$, $q = -1$,$r = 1$, $k = 1$ and $\beta = -1$. The profiles show the bright shaped solitons that are confirmed through the cross-sectional 2D plots displayed in Fig. 5(b1)–(b3). The cross-sectional plots are prepared by taking a transect $x = 0$ from Fig. 5(a1)–(a3). At $s = 1$, it is realized from Fig. 5(a1) that the soliton corresponding to $u_{13}(x,t)$ is of bright shape with a width larger than that of the soliton corresponding to $u_{14}(x,t)$, but both of them have the same amplitude. As s increases ($s = 3,5$), one can observe from Fig. 5(a2)–(a3) that the width of the wave corresponding to$u_{13}(x,t)$ gradually decreases, but the width remains unchanged for the wave corresponding to $u_{14}(x,t)$. At the end, both of them reach to the identical shape of a bright soliton. It can be justified by their 2D plots, which are shown in Fig. 5(b1)–(b3). The roles of k, s, and β on the motion of the two moving two-waves of u_{13} and u_{14} are displayed in Fig. 6(a)–(c), respectively. With increasing wave number k, the 2D profile of u_{13} decreases, but the reverse phenomena can be found for u_{14} that of u_{13}. For other parameters s and β, the profile of u_{14} significantly higher than that of u_{13}, but the profile remains fixed for u_{13}. The results are found to be consistent with the 3D profiles of u_{13} and u_{14}. The remaining solutions explored via the NAEM indicate the bright, dark, singular shaped solitons, which are not displayed for the sake of simplicity.

Based on the graphical analysis of the mKM and NAEM produced solutions, it is revealed that the increase of s can lead to the increase in the soliton velocities under the condition of $\alpha = \beta$, but the soliton amplitudes remain unchanged. The collisions between the two solitons in both two modes are analyzed with the help of graphical analysis. Therefore, it is clear from the graphical outputs of the mKM and NAEM produced solutions that the methods can be used to solve any two-mode nonlinear PDE to produce new dual-wave solutions.

Conclusions and future recommendations

The findings of this work based on the explored dual shape wave solutions are summarized as follows.

(i) Bright shaped soliton solutions are attained through the mKM,
(ii) Bright, dark, periodic, singular-periodic, and singular shaped soliton solutions are produced when the NAEM is adopted, and
(iii) The roles of the phase velocity (s), wave number (k) and dispersion parameter (β) are explained graphically that can accelerate the motion of the dual-wave.

The nature of the dual-wave solutions is discussed by their 3D and 2D graphics. It can be found that both waves (right/left mode) of the acquired solutions have the same shape (bright, dark, periodic, singular-periodic, and singular), but they only move the direction. It is also found that two waves are seemed to be one when s increases excepting periodic shaped solitons. Based on the summarized results (i)–(iii), it can be concluded that the NAEM is more efficient over the mKM to explore new dual-wave solutions. The mentioned methods can be applied to any dual-mode nonlinear PDEs in any physical systems to explore new dual-wave solutions. Our future work would be concentrated towards investigating the new dual-wave solutions by using different analytical, semi-analytical, and numerical methods to the TmSK equation. The fractional derivative will also be considered to this equation to derive such types of solutions.

CRediT authorship contribution statement

Dipankar Kumar: Conceptualization, Formal analysis, Methodology, Project administration, Resources, Writing - original draft. **Choonkil Park:** Funding acquisition, Methodology, Resources, Software, Supervision, Validation, Writing - review editing. **Nishat Tamanna:** Data curation, Investigation, Resources, Validation, Writing - review editing. **Gour Chandra Paul:** Formal analysis, Methodology, Software, Writing - original draft. **M.S. Osman:** Conceptualization, Funding acquisition, Investigation, Methodology, Project administration, Resources, Software, Supervision, Validation, Visualization, Writing - review editing.

Declaration of Competing Interest

The authors declare that they have no known competing financial interests or personal relationships that could have appeared to influence the work reported in this paper.

Acknowledgement

The study is partially supported by the Ministry of Science and Technology, Government of the People's Republic of Bangladesh, by providing National Science and Technology (NST) fellowship under grant Number No. 39.00.0000.012.002.04.19-06 to the third author acknowledges this support.

References

[1] Zwillinger D. Handbook of differential equations. New York: Academic Press; 1992.
[2] Osman MS, Rezazadeh H, Eslami M, Neirameh A, Mirzazadeh M. Analytical study of solitons to benjamin-bona-mahony-peregrine equation with power law nonlinearity by using three methods. University Politehnica Bucharest Scientific Bull-Ser A 2018;80(4):267–78.
[3] Kumar D, Kaplan M. Application of the modified Kudryashov method to the generalized Schrödinger-Boussinesq equations. Opt Quant Electron 2018;50(9):329.
[4] Srivastava HM, Baleanu D, Machado JAT, Osman MS, Rezazadeh H, Arshed S, Günerhan H. Traveling wave solutions to nonlinear directional couplers by modified Kudryashov method. Phys Scr 2020;95(7).
[5] Kumar D, Darvishi MT, Joardar AK. Modified Kudryashov method and its application to the fractional version of the variety of Boussinesq-like equations in shallow water. Opt Quant Electron 2018;50(3):128.
[6] Kaplan M, Bekir A, Akbulut A. A generalized Kudryashov method to some nonlinear evolution equations in mathematical physics. Nonlinear Dyn 2016;85(4):2843–50.
[7] Khater MM, Kumar D. New exact solutions for the time fractional coupled Boussinesq-Burger equation and approximate long water wave equation in shallow water. J Ocean Eng Sci 2017;2(3):223–8.
[8] Hassan MM, Abdel-Razek MA, Shoreh AH. New exact solutions of some (2+1)-dimensional nonlinear evolution equations via extended Kudryashov method. Rep Math Phys 2014;74(3):347–58.
[9] Liu CS. Trial equation method to nonlinear evolution equations with rank inhomogeneous: mathematical discussions and its applications. Commun Theor Phys 2006;45:219–23.
[10] Zhou Q, Ekici M, Sonmezoglu A, Mirzazadeh M, Eslami M. Optical solitons with Biswas-Milovic equation by extended trial equation method. Nonlinear Dyn 2016;84(4):1883–900.
[11] Cheng W, Xu T. N-th Bäcklund transformation and soliton-cnoidal wave interaction solution to the combined KdV-negative-order KdV equation. Appl Math Lett 2019;94:21–9.
[12] Cheng W, Qiu D, Xu T. Residual symmetry, n th Bäcklund transformation, and soliton-cnoidal wave interaction solution for the combined modified KdV-negative-order modified KdV equation. Math Methods Appl Sci 2020;43(3):1253–66.
[13] Cheng W, Qiu D, Xu T. Multiple residual symmetries and soliton-cnoidal wave interaction solution of the (2+ 1)-dimensional negative-order modified Calogero-Bogoyavlenskii-Schiff equation. Eur Phys J Plus 2020;135(1):1–12.
[14] Biswas A, Yildirim Y, Yasar E, Zhou Q, Moshokoa SP, Belic M. Optical solitons for Lakshmanan-Porsezian-Daniel model by modified simple equation method. Optik 2018;160:24–32.
[15] Kumar D, Hosseini K, Samadani F. The sine-Gordon expansion method to look for the traveling wave solutions of the Tzitzéica type equations in nonlinear optics. Optik 2017;149:439–46.
[16] Ali KK, Osman MS, Abdel-Aty M. New optical solitary wave solutions of Fokas-Lenells equation in optical fiber via Sine-Gordon expansion method. Alexandria Eng J 2020;59:1191–6.
[17] Kumar D, Joardar AK, Hoque A, Paul GC. Investigation of dynamics of nematicons in liquid crystals by extended sinh-Gordon equation expansion method. Opt Quant Electron 2019;51(7):212.
[18] Kumar D, Manafian J, Hawlader F, Ranjbaran A. New closed form soliton and other solutions of the Kundu-Eckhaus equation via the extended sinh-Gordon equation expansion method. Optik 2018;160:159–67.
[19] Bilige S, Chaolu T, Wang X. Application of the extended simplest equation method to the coupled Schrödinger-Boussinesq equation. Appl Math Comput 2013;224:517–23.
[20] Rezazadeh H. New solitons solutions of the complex Ginzburg-Landau equation with Kerr law nonlinearity. Optik 2018;167:218–27.
[21] Abdel-Gawad HI, Osman MS. On the variational approach for analyzing the stability of solutions of evolution equations. Kyungpook Math J 2013;53(4):661–80.
[22] Osman MS, Rezazadeh H, Eslami M. Traveling wave solutions for (3+ 1) dimensional conformable fractional Zakharov-Kuznetsov equation with power law nonlinearity. Nonlinear Eng 2019;8(1):559–67.
[23] Abdel-Gawad HI, Osman M. Exact solutions of the Korteweg-de Vries equation with space and time dependent coefficients by the extended unified method. Indian J Pure Appl Math 2014;45(1):1–12.
[24] Abdel-Gawad HI, Elazab NS, Osman M. Exact solutions of space dependent Korteweg-de Vries equation by the extended unified method. J Phys Soc Jpn 2013;82(4).
[25] Osman MS, Baleanu D, Adem AR, Hosseini K, Mirzazadeh M, Eslami M. Double-wave solutions and Lie symmetry analysis to the (2+ 1)-dimensional coupled Burgers equations. Chin J Phys 2020;63:122–9.
[26] Akbar MA, Ali NHM, Tanjim T. Outset of multiple soliton solutions to the nonlinear Schrodinger equation and the coupled Burgers equation. J Phys Commun 2019;3(2019).
[27] Khalid M, Khan FS. A new approach for solving highly nonlinear partial differential equations by successive differentiation method. Math Methods Appl Sci 2017;40(16):5742–9.
[28] Wazwaz AM. The decomposition method applied to systems of partial differential equations and to the reaction-diffusion Brusselator model. Appl Math Comput 2000;110(2–3):251–64.
[29] Liu JG, Zhu WH, Osman MS, Ma WX. An explicit plethora of different classes of interactive lump solutions for an extension form of 3D-Jimbo-Miwa model. Eur Phys J Plus 2020;135(6):412.
[30] Ma YL. N-solitons, breathers and rogue waves for a generalized Boussinesq equation. Int J Comput Math 2020;97(8):1648–61.
[31] Li BQ. Loop-like kink breather and its transition phenomena for the Vakhnenko equation arising from high-frequency wave propagation in electromagnetic physics. Appl Math Lett 2021;112.
[32] Liu JG, Osman MS, Zhu WH, Zhou L, Baleanu D. The general bilinear techniques for studying the propagation of mixed-type periodic and lump-type solutions in a homogenous-dispersive medium. AIP Adv 2020;10(10).
[33] Ismael HF, Bulut H, Park C, Osman MS. M-lump, N-soliton solutions, and the collision phenomena for the (2+ 1)-dimensional Date-Jimbo-Kashiwara-Miwa equation. Results Phys 2020;19.
[34] Tahir M, Awan AU, Osman MS, Baleanu D, Alqurashi MM. Abundant periodic wave solutions for fifth-order Sawada-Kotera equations. Results Phys 2020;17.
[35] Osman MS, Inc M, Liu JG, Hosseini K, Yusuf A. Different wave structures and stability analysis for the generalized (2+ 1)-dimensional Camassa-Holm-Kadomtsev-Petviashvili equation. Phys Scr 2020;95(3).
[36] Lepik Ü. Numerical solution of evolution equations by the Haar wavelet method. Appl Math Comput 2007;185(1):695–704.
[37] Kanth AR, Reddy YN. Higher order finite difference method for a class of singular boundary value problems. Appl Math Comput 2004;155(1):249–58.
[38] Jiang Y, Ma J. High-order finite element methods for time-fractional partial differential equations. J Comput Appl Math 2011;235(11):3285–90.
[39] Ma YL. Interaction and energy transition between the breather and rogue wave for a generalized nonlinear Schrödinger system with two higher-order dispersion operators in optical fibers. Nonlinear Dyn 2019;97(1):95–105.
[40] Ma YL, Li BQ. Interactions between soliton and rogue wave for a (2+ 1)-dimensional generalized breaking soliton system: hidden rogue wave and hidden soliton. Comput Math Appl 2019;78(3):827–39.
[41] Guan WY, Li BQ. Mixed structures of optical breather and rogue wave for a variable coefficient inhomogeneous fiber system. Opt Quant Electron 2019;51(11):352.
[42] Ma YL, Li BQ. Mixed lump and soliton solutions for a generalized (3+ 1)-dimensional Kadomtsev-Petviashvili equation. AIMS Math 2020;5(2):1162.
[43] Li BQ, Ma YL. Extended generalized Darboux transformation to hybrid rogue wave and breather solutions for a nonlinear Schrödinger equation. Appl Math Comput 2020;386.
[44] Korsunsky SV. Soliton solutions for a second order KdV equation. Phys Lett A 1994;185(2):174–6.
[45] Xiao ZJ, Tian B, Zhen HL, Chai J, Wu XY. Multi-soliton solutions and Bäcklund transformation for a two-mode KdV equation in a fluid. Waves Random Complex Medium 2017;27(1):1–14.
[46] Wazwaz AM. A two-mode modified KdV equation with multiple soliton solutions. Appl Math Lett 2017;70:1–6.
[47] Wazwaz AM. Two wave mode higher order modified KdV equations: essential conditions for multiple soliton solutions to exist. Int J Numer Methods Heat Fluid Flow 2017;27(10):2223–30.
[48] Wazwaz AM. Two-mode fifth order KdV equations: necessary conditions for multiple-soliton solutions to exist. Nonlinear Dyn 2017;87(3):1685–91.
[49] Ali M, Alquran M, Jaradat I, Baleanu D. Stationary wave solutions for new developed two-waves' fifth-order Korteweg-deVries equation. Adv Difference Equations 2019;2019(1):263.
[50] Wazwaz AM. Two-mode Sharma-Tasso-Olver equation and two-mode fourth-order Burgers equation: multiple kink solutions. Alexandria Eng J 2018;57(3):1971–6.
[51] Wazwaz AM. A two-mode Burgers equation of weak shock waves in a fluid: multiple kink solutions and other exact solutions. Int J Appl Comput Math 2017;3(4):3977–85.
[52] Alquran M, Jaradat HM, Syam MI. A modified approach for a reliable study of new nonlinear equation: two-mode Korteweg-deVries-Burgers equation. Nonlinear Dyn 2018;91(3):1619–26.
[53] Jaradat I, Alquran M, Ali M. A numerical study on weak-dissipative two-mode perturbed Burgers' and Ostrovsky models: right-left moving waves. Eur Phys J Plus 2018;133(4):164.
[54] Wazwaz AM. A study on a two-wave mode Kadomtsev-Petviashvili equation: conditions for multiple soliton solutions to exist. Math Methods Appl Sci 2017;40(11):4128–33.
[55] Irwaq IA, Alquran M, Jaradat I, Baleanu D. New dual-mode Kadomtsev-Petviashvili model with strong-weak surface tension: analysis and application. Adv Differ Equations 2018;2018(1):433.
[56] Jaradat HM, Alquran M, Syam MI. A reliable study of new nonlinear equation: two-mode Kuramoto-Sivashinsky. Int J Appl Comput Math 2018;4(2):64.
[57] Alquran M, Yassin O. Dynamism of two-mode's parameters on the field function for third-order dispersive Fisher: application for fibre optics. Opt Quant Electron 2018;50(9):354.
[58] Jaradat A, Noorani MSM, Alquran M, Jaradat HM. Construction and solitary wave solutions of two-mode higher-order Boussinesq-Burger system. Adv Differ Equations 2017;2017(1):376.

[59] Jaradat I, Alquran M, Momani S, Biswas A. Dark and singular optical solutions with dual-mode nonlinear Schrödinger's equation and Kerr-law nonlinearity. Optik 2018;172:822–5.
[60] Jaradat HM, Syam M, Alquran M. A two-mode coupled Korteweg-de Vries: multiple-soliton solutions and other exact solutions. Nonlinear Dyn 2017;90(1): 371–7.
[61] Syam M, Jaradat HM, Alquran M. A study on the two-mode coupled modified Korteweg-de Vries using the simplified bilinear and the trigonometric-function methods. Nonlinear Dyn 2017;90(2):1363–71.
[62] Alquran M, Jaradat I, Baleanu D. Shapes and dynamics of dual-mode Hirota-Satsuma coupled KdV equations: exact traveling wave solutions and analysis. Chin J Phys 2019;58:49–56.
[63] Kumar VS, Rezazadeh H, Eslami M, Izadi F, Osman MS. Jacobi elliptic function expansion method for solving KdV equation with conformable derivative and dual-power law nonlinearity. Int J Appl Comput Math 2019;5(5):127.
[64] Liu JG, Osman MS, Wazwaz AM. A variety of nonautonomous complex wave solutions for the (2+ 1)-dimensional nonlinear Schrödinger equation with variable coefficients in nonlinear optical fibers. Optik 2019;180:917–23.
[65] Ali KK, Abd El Salam MA, Mohamed EM, Samet B, Kumar S, Osman MS. Numerical solution for generalized nonlinear fractional integro-differential equations with linear functional arguments using Chebyshev series. Adv Differ Equations 2020; 2020(1):494.